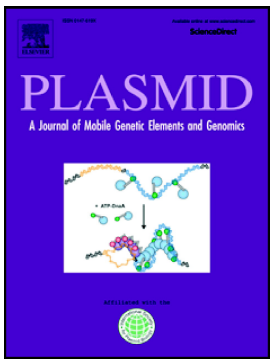

Delineation of the integrase-attachment and origin-of-transfer regions of the symbiosis island ICEMlSymR7A

Callum J. Verdonk, John T. Sullivan, Kate M. Williman, Leila Nicholson, Tahlia R. Bastholm, Michael F. Hynes, Clive W. Ronson, Charles S. Bond, Joshua P. Ramsay

PII: S0147-619X(18)30152-5
DOI: https://doi.org/10.1016/j.plasmid.2019.102416
Article Number: 102416
Reference: YPLAS 102416

To appear in: *Plasmid*

Received date: 14 December 2018
Revised date: 12 April 2019
Accepted date: 7 May 2019

Please cite this article as: C.J. Verdonk, J.T. Sullivan, K.M. Williman, et al., Delineation of the integrase-attachment and origin-of-transfer regions of the symbiosis island ICEMlSymR7A, Plasmid, https://doi.org/10.1016/j.plasmid.2019.102416

Delineation of the integrase-attachment and origin-of-transfer regions of the symbiosis island ICE*Ml*Sym^{R7A}

Callum J. Verdonk[1,2], John T. Sullivan[3], Kate M. Williman[3], Leila Nicholson[3], Tahlia R. Bastholm[2], Michael F. Hynes[4], Clive W. Ronson[3], Charles S. Bond[1] and Joshua P. Ramsay[2]*

[1] School of Molecular Sciences, University of Western Australia, Perth, WA, Australia

[2] School of Pharmacy and Biomedical Sciences and Curtin Health Innovation Research Institute, Curtin University, Perth, WA, Australia

[3] Department of Microbiology and Immunology, University of Otago, Dunedin, New Zealand

[4] Department of Biological Sciences, University of Calgary, Calgary, Canada

* To whom correspondence should be addressed. Email: josh.ramsay@curtin.edu.au

Keywords: Integrative and Conjugative Element; origin of transfer; integrase; excisionase; ICE*Ml*Sym^{R7A}

ABSTRACT

Integrative and conjugative elements (ICEs) are chromosomally-integrated mobile genetic elements that excise from their host chromosome and transfer to other bacteria via conjugation. ICE*Ml*Sym^{R7A} is the prototypical member of a large family of "symbiosis ICEs" which confer upon their hosts the ability to form a nitrogen-fixing symbiosis with a variety of legume species. Mesorhizobial symbiosis ICEs carry a common core of mobilisation genes required for integration, excision and conjugative transfer. IntS of ICE*Ml*Sym^{R7A} enables recombination between the ICE*Ml*Sym^{R7A} attachment site *attP* and the 3' end of the *phe*-tRNA gene. Here we identified putative IntS *attP* arm (P) sites within the *attP* region and demonstrated that the outermost P1 and P5 sites demarcated the minimal region for efficient IntS-mediated integration. We also identified the ICE*Ml*Sym^{R7A} origin-of-transfer (*oriT*) site directly upstream of the relaxase-gene *rlxS*. The ICE*Ml*Sym^{R7A} conjugation system mobilised a plasmid carrying the cloned *oriT* to *Escherichia coli* in an *rlxS*-dependent manner. Surprisingly, an in-frame, markerless deletion mutation in the ICE*Ml*Sym^{R7A} recombination directionality factor (excisionase) gene *rdfS*, but not a mutation in *intS*, abolished mobilisation, suggesting the *rdfS* deletion tentatively has downstream effects on conjugation or its regulation. In summary, this work defines two critical *cis*-acting regions required for excision and transfer of ICE*Ml*Sym^{R7A} and related ICEs.

1. INTRODUCTION

Integrative and Conjugative Elements (ICEs) are chromosomally-integrated elements that transfer between bacteria by conjugation (1-3). ICEs are likely the most abundant conjugative element in prokaryotic genomes and carry diverse genetic cargo, which can confer phenotypes such as antimicrobial-resistance, virulence, metabolism and the capacity to enter symbiotic associations with eukaryotes (4-10). After entry of an ICE into a recipient cell, integration into the host chromosome occurs through the actions of an ICE-encoded site-specific recombinase; termed an integrase (11, 12). Integrases belong to either the tyrosine or serine recombinase families; defined by the conserved nucleophilic amino acid that becomes covalently bonded to a DNA strand during the recombination reaction (11).

The recombination events mediated by integrases have largely been defined by studies performed on phages (11-14). Integrases form nucleoprotein complexes consisting of a homodimer structures bound to *cis*-acting DNA regions called attachment (*att*) sites present in the phage and host chromosomes (11). During chromosomal integration, an *attP* site present on the circularised phage genome, is recombined with the host chromosome attachment site *attB*. Upon integration, the integration junctions termed *attL* and *attR* are formed. Each *att* site contains a "catalytic core" site where strand exchange occurs. *att* sites also contain "arm" or "P" sites which flank the core. The P sites facilitate structural organisation of the integrase-DNA complex during recombination (11, 15-17). Recombinases are heterobivalent in that the N-terminal region binds the P sites and the C-terminal region interacts with the *att* core sequence where recombination occurs. During recombination the nucleophilic residue within the C-terminus becomes covalently fused to a DNA strand. An incoming DNA strand then displaces the residue reforming an intact DNA strand resulting in formation of a double-stranded cruciform DNA structure known as a Holliday junction intermediate. A second round of cleavage, strand exchange and ligation resolves this structure to produce the recombination end products (3, 18, 19).

Integrated ICEs are flanked by hybrid *attL* and *attR* sites and the two core sites form a direct repeat bordering the inserted ICE. For both phages and ICEs, excision is catalysed by the integrase, but often an additional factor known as an excisionase or recombination directionality factor (RDF) is required. Excisionases have been shown to bind and bend *att* DNA, shifting the favoured direction of integrase-mediated recombination towards the excision reaction (*attL* + *attR* > *attP* + *attB*) (11, 20). Certain excisionases, particularly the subset *cox* family, have bifunctional roles as transcriptional regulators (12, 21-27). The P2 phage excisionase Cox stimulates the lytic cycle by blocking

transcription of repressor gene *cI*, in addition to its roles as an *att*-binding prophage excision stimulator (25, 26).

ICE*Ml*Sym^{R7A} is a 502-kb ICE which encodes genes required to form a nitrogen-fixing symbiosis with legumes of the genus *Lotus* (9, 28)**.** Subsequent to the discovery of ICE*Ml*Sym^{R7A}, numerous other mobile symbiosis ICEs have been identified within mesorhizobial strains that confer the ability to form symbioses with a variety of legumes including *Biserrula* and Chickpea (29-31). Recently, more complex tripartite symbiosis ICEs have been discovered, which carry a similar core gene complement to ICE*Ml*Sym^{R7A} but upon integration in a new host they fragment into three physically separate regions within the host chromosome through the action of two additional integrases (31, 32).

ICE*Ml*Sym^{R7A} is a monopartite ICE that integrates into the single *phe*-tRNA gene of the *Mesorhizobium loti* R7A chromosome (9, 20), a feature common to symbiosis ICEs found within mesorhizobia including the tripartite ICEs (31). Integration requires the integrase IntS, a tyrosine recombinase related to the P4 bacteriophage integrase family (20). The ICE*Ml*Sym^{R7A} *attP* site contains a 17-bp DNA sequence identical to the last 17-bp of the *phe*-tRNA gene and integration of ICE*Ml*Sym^{R7A} into this *attB* site reconstitutes the *phe*-tRNA gene within the newly-formed *attL* site (9, 20). We have previously demonstrated that a synthetic "mini-ICE" carrying only *intS* and *attP* integrates into the *phe*-tRNA gene in R7ANS; a derivative of R7A from which ICE*Ml*Sym^{R7A} was cured (20). The ICE*Ml*Sym^{R7A} RDF, RdfS, is a putative member of the MerR superfamily of winged helix-turn-helix (wHTH) DNA-binding proteins (12, 33, 34). Deletion of *rdfS* abolishes excision of ICE*Ml*Sym^{R7A}, while overexpression of *rdfS* leads to loss of ICE*Ml*Sym^{R7A}, producing the non-symbiotic derivative strain R7ANS (20). Expression of *rdfS* in R7ANS carrying an integrated copy of the mini-ICE stimulated its excision and subsequent loss, suggesting *rdfS* and *intS* together are sufficient for ICE*Ml*Sym^{R7A} excision (20).

Unlike most RDF genes, which are generally positioned directly adjacent to their cognate integrase gene (12), *rdfS* is located within a highly conserved symbiosis-ICE gene cluster, containing conjugation-associated genes including *traF* (encoding a putative prepilin peptidase), a lytic transglycosylase, a VirD2-like conjugative relaxase gene *rlxS* and the putative ICE*Ml*Sym^{R7A} origin-of-transfer (*oriT*) region (20, 28). *oriT* sites are *cis*-acting regions that generally contain inverted repeats and a *nic*/core site targeted by a relaxase protein. Relaxases, often in association with other components, form a protein-DNA complex with the *oriT* called the relaxosome. Within the relaxosome, the relaxase nicks DNA within the *nic* core site and remains covalently attached to the 5'

phosphate of the nicked strand, after which it pilots DNA to the type-IV secretion system for conjugative transfer (35, 36). Relaxosomes often include accessory proteins required for specific recognition of the *oriT* and/or stimulation of *oriT* cleavage (37-39). Mutation of ICE*Ml*Sym^{R7A} *rlxS* abolishes transfer of ICE*Ml*Sym^{R7A}. Moreover, *rlxS* is also required for maintenance of ICE*Ml*Sym^{R7A} during excision, suggesting relaxase-mediated rolling-circle replication contributes to ICE*Ml*Sym^{R7A} maintenance when in the excised form (20).

In this work, we further define two *cis*-acting DNA sites of ICE*Ml*Sym^{R7A}, the IntS attachment site *attP* and the *oriT* site. The minimal *attP* site contained five copies of a directly repeated sequence motif in a pattern resembling the arm sites of other characterised *attP* regions. Removal of a single proximal or distal "P" site severely hampered IntS-mediated integration. Conjugative mobilisation experiments were used to confirm the ICE*Ml*Sym^{R7A} origin-of-transfer (*oriT*) region was located upstream of the *rlxS* gene. Unexpectedly, an intact *rdfS* gene was required for mobilisation, suggesting this mutation has an effect on the expression of the ICE*Ml*Sym^{R7A} conjugation system.

2. MATERIAL AND METHODS

2.1 Strains and growth conditions

Strains used in this study are listed in **Supplemental Table 1**. *M. loti* strains were cultured at 28^{o}C or 30^{o}C in Tryptone Yeast (TY) media (0.3% *w/v* yeast extract, 0.5% *w/v* tryptone, 0.6% *v/v* $CaCl_2$) or in glucose rhizobium defined medium (G/RDM) (40) supplemented with vitamins as described previously (20). *Escherichia coli* DC10B (41) cultures were grown in Lysogeny broth (LB) at 37^{o}C. Media was supplemented with antibiotics where required at the following concentrations: 2.0 µg/mL (*M. loti*) and 5.0 µg/mL (*E. coli*) tetracycline, 50 µg/mL gentamicin and 50 µg/mL ampicillin.

2.2 Molecular biology and cloning

Plasmid construction is detailed in **Supplemental Table 1** and oligonucleotides and QPCR probes used are described in **Supplemental Table 2**. QPCR was carried using the ViiA 7 Real-time PCR system (Applied Biosystems) in 20-µl reactions using the SensiFAST Probe Lo-ROX Kit (Bioline), using the standard-speed running conditions (i.e. non-fast). DNA was extracted from stationary-phase non-IPTG induced TY cultures (64 h) using PrepMan Ultra (ThermoFisher) reagent as previously described (20). Primers and probes used were purchased from Integrated DNA Technologies (IDT - Singapore) and probes were modified with a 5' FAM fluorophore and 3' ZEN quencher. The *melR* gene probe was lengthened to increase binding and compensate for the lack of a minor-groove-binder ligand on the IDT probes. The primer/probe combinations exhibited QPCR efficiencies of 2.04, 2.09 and 2.03 for *attP*, *attB* and *melR*, respectively. Reactions were normalised using the standard template as previously described (20).

2.3 Integration assays for attP*-carrying plasmids*

Two-hundred nanogram aliquots of plasmid DNA were electroporated into electrocompetent R7ANS(pJJ611) cells as previously described (42). Cells were recovered in 1 mL TY broth with shaking at 28°C for 3 hours. Serial dilutions were then plated on G/RDM containing vitamins (thiamin, biotin and nicotinate) (20) and gentamicin. Colonies were enumerated after 5 days of growth at 28°C. pFUS conjugation experiments of *E. coli* ST18 and *M. loti* R7ANS(pJJ611) were performed as described in section 2.4. Confirmation of pFUS vector integration sites were done by PCR and sequencing (primers used listed in **Supplemental Table 2**).

2.4 Conjugative mobilisation experiments

M. loti donor strains carrying pFAJ2013 (strains used are listed in **Supplemental Table 1**) (20) and the *E. coli* recipient DC10B were grown to stationary phase (OD_{600} 0.8-1.0) in 5 mL TY (R7A) or LB-broth (DC10B). Five-hundred microlitres of *M. loti* TY culture were pelleted and resuspended in 500 µL *E. coli* DC10B LB culture and centrifuged for an additional 2 minutes at 17,000 g. The pellet was resuspended in 100 µL TY broth. Thirty-microlitres of the cell mixture spotted in triplicate onto TY agar media and incubated at 30^{o}C overnight. Strains containing pSRKKm or pSRKrdfS were spot plated on TY agar media. Mobilisation experiments with R7AΔ*rdfS*(pFAJ2013)(pSRKrdfS) were carried out both with and without 1 mM IPTG, however no mobilisation was observed in either experiment. Spots were recovered and resuspended in 1 mL sterile water and serial diluted 10-fold to 1 x 10^{-9}. One-hundred microlitre aliquots were plated onto LB agar containing tetracycline and incubated overnight at 37°C, and colonies were enumerated. Controls consisting of the donor strains only were prepared similarly, with 500 µL culture resuspended in 100 µL TY broth and 30 µl spots grown overnight at 30^{o}C on TY agar media.

2.5 Bioinformatic analyses of attP *and* oriT *regions.*

The ICE*Ml*Sym^{R7A} sequence is available from GenBank accession AL672111.1 (28). A 352-bp putative *attP* region (assembled from 501647-501801[*attR*] and 1-157[*attL*]) was used in MEME (43)(version 5.0.2) alignments with non-mesohizobial sequences identified by PSI-BLAST (44) as described in section 3.1. GenBank accessions used; *Magnetospirillum* sp. (FXXN01000020.1), *Marinicaulis flavus* (PJCH01000010.1), *Nitrospirillum amazonense* (AFBX01000767.1), *Acidisphaera* sp. (CP029176.1), Rhizobiales sp. (PIGG01000031.1), *Prosthecomicrobium hirschii* (LJYW01000001.1), *Sphingomonas* sp. (CH959307.1) and *Rhodopseudomonas palustris* (CP000301.1). The putative 352-bp *attP* region was also submitted to MEME with BLAST-identified *Mesorhizobium* spp. *phe*-tRNA-adjacent intergenic regions (GenBank accessions: CCNB01000043.1, AYWT01000014.1, KI421454.1, MDLH01000001.1, CAAF010000028.1, AYVN01000010.1, CCNA01000045.1, MDFL01000146.1, NPKJ01000019.1, PZJX01000011.1, FNEE01000009.1, NNRI01000015.1, AHAM01000208.1 and MZXV01000055.1) to confirm the presence of the identified P-site motif.

ICE*Ml*Sym^{R7A} putative *oriT* sequence was collected from the upstream region of *rlxS* (*msi106*) (133491-133680) and used in PSI-BLAST investigations described in section 3.2. GenBank accessions used; *Sphingobium lactosutens* (ATDP01000088.1), *Oceanibaculum nanhaiense* (MPOB01000010.1), *Phaeospirillum fulvum* (FNWO01000021.1), *Rhodospirillum photometricum* (HE663493.1), *Thalassospira xiamenensis* (LPXL01000008.1), *Niveispirillum cyanobacteriorum* (CP025612.1) and *Erythrobacter xanthus* (QXFM01000025.1). HMMER hmmscan described in section 3.2 used hmm

profiles downloaded from https://github.com/gem-pasteur/Macsyfinder_models/tree/master/models/Conjugation/profiles.

3. RESULTS

3.1 Identification of the minimal ICE*Ml*Sym^{R7A} *attP* site required for integration

intS is located directly downstream of the ICE*Ml*Sym^{R7A} *attL* site, which also forms part of the *attP* site on the circularised element. To identify potential IntS P sites within the ICE*Ml*Sym^{R7A} *att* sites, we initially used PSI-BLASTP (44) searches to identify divergent IntS homologues outside the *Mesorhizobium* genus. Nucleotide sequences corresponding to each IntS-homologue gene were inspected to determine if the integrase was preceded by a tRNA gene. Intergenic regions between each tRNA and *intS* homologue were collected and analysed along with the ICE*Ml*Sym^{R7A} *attL* region using the MEME motif identifier software (43, 45). MEME was set to search for multiple repetitions (per sequence) of a 5-20-bp motif. A motif with consensus "TGKTGGTATC" was present as 2-3 direct repeats in each of the putative *attL* sequences (**Fig 1A**). Inspection of the ICE*Ml*Sym^{R7A} *attP* revealed two additional copies of this motif upstream of the core region (on *attP* / *attR*). The five sites were named P1-P5 (**Fig. 1B**)**.** All five instances of the suspected P-site motif were conserved on the IntS *attP* regions of *Mesorhizobium* spp. strains: WSM1284, WSM1497, NZP2037 and WSM1271 (**Fig. 1B**).

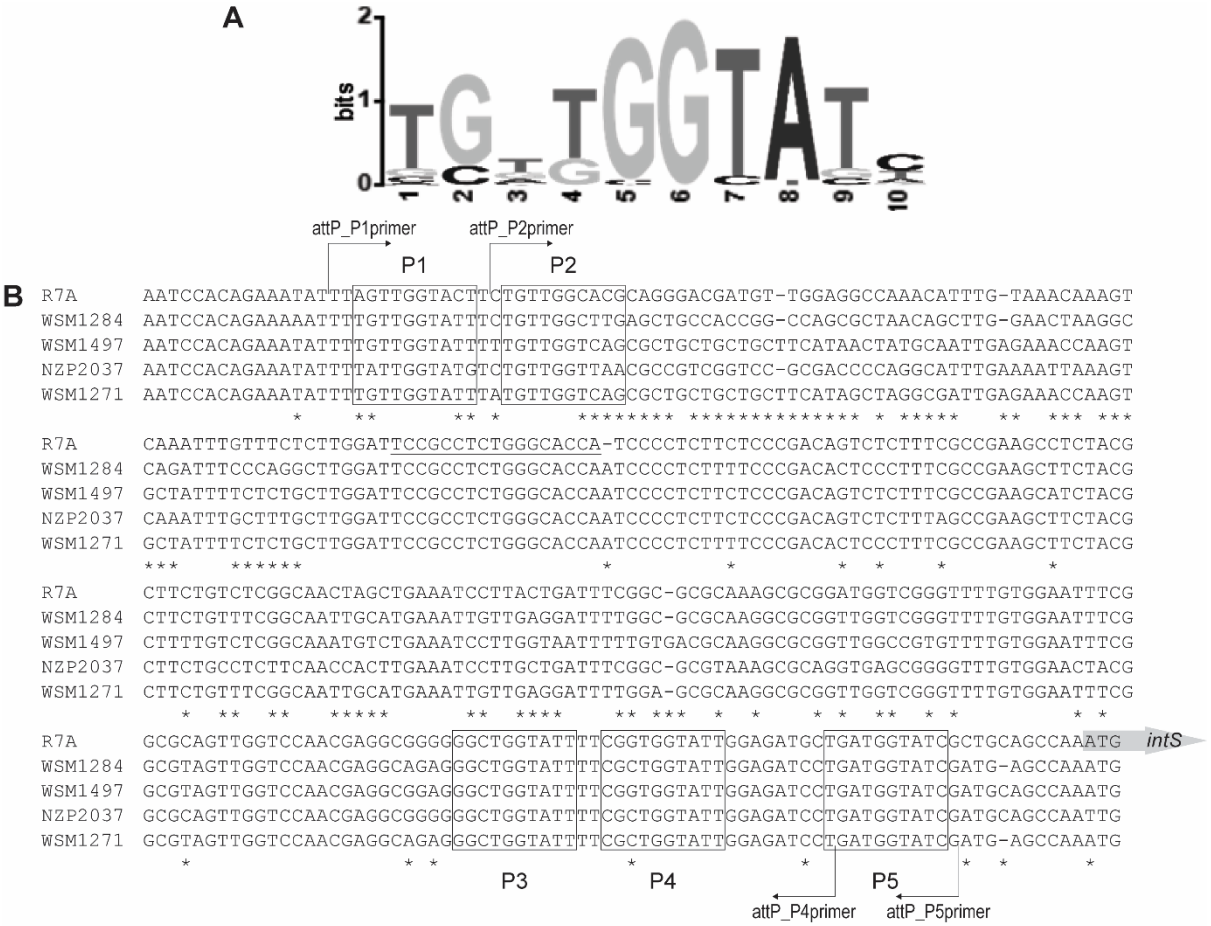

Fig. 1. The ICE*Ml*Sym^{R7A} *attP* site. (A) Putative P-site sequence motif derived from an alignment of *attL* regions corresponding to divergent IntS homologues (see Section 2.5). (B) ICE*Ml*Sym^{R7A} *attP* sequence aligned (using MAFFT (46)) with the *attP* regions of *Mesorizobium* spp. WSM1284 (accession: CP015064.1), WSM1497 (accession: CP021070.1), NZP2037 (accession: CP016079.1) and WSM1271 (accession: CP002447.1) Asterisks (*) denotes alignment difference from consensus. Putative P-sites P1-P5 are boxed. ICE*Ml*Sym^{R7A} 17-bp core-containing region is underlined. The 5' start site of primers used to PCR-amplify the *attP* regions used in pFUS2 integration assays are shown as arrows.

intS and *attP* can function together to recombine *attP* and *attB* when cloned on separate plasmids. An introduced suicide vector carrying a 628-bp *attP* region (pJJ610) is efficiently integrated into the *phe*-tRNA gene, but only in the presence of a functional *intS* expressed by a coresident plasmid pJJ611 (20)**.** We extended this approach here to define the minimal *attP* region. A smaller 283-bp region of *attP* containing only the P1-P5 region was cloned into the gentamicin-resistance suicide plasmid pFUS2, producing pFUSP1-P5. pFUS plasmids lacking either P1, P5 or both P1 and P5, were additionally constructed. Each construct was then transferred by conjugation from *E. coli* ST18 (47) to R7ANS(pJJ611). Apparent transfer produced rates for the P1-P5 construct were on average 3.8 x 10^{-3} exconjugants per donor, but experiments using the pFUS2 clones lacking the outermost P1 or P5 sites were reduced 190- and 140-fold, respectively (**Table 1**). No colonies were isolated following transfer of the clone lacking both P1 and P5, suggesting removal of both sites abolished IntS-mediated integration. The *attR* sites formed by examples of the three integrated pFUS2 constructs were amplified by PCR and sequenced, which confirmed the constructs integrated downstream of the *phe*-tRNA gene (9, 20). We additionally electroporated the same pFUS2 constructs into R7ANS(pJJ611), which produced a similar pattern of results. Therefore, these experiments both defined the minimal *attP* site for IntS and suggested that the outermost P1 and P5 sites are required for efficient IntS-mediated recombination.

Table 1. Conjugation and electroporation assays for IntS-mediated *attP* integration.

attP region†	Apparent conjugation rate§	Apparent electroporation efficiency cfu/ml/ng DNA
P1-P5	3.8 x 10^{-3} ± 8.8 x 10^{-4}	935 ± 420
P1-P4	1.9 x 10^{-5} ± 3.0 x 10^{-6}	3.1 ± 1.3
P2-P5	2.5 x 10^{-5} ± 8.7 x 10^{-6}	4.0 ± 2.2
P2-P4	ND§	0
none	ND§	0

†*attP* regions cloned into non-replicative plasmid pFUS2 and conjugated or electroporated into R7ANS(pJJ611).

‡Conjugation rates are expressed as exconjugants per donor and all data are the average of three replicates of the entire experiment.

§Limit of detection for conjugation approximately 3 x 10^{-8} exconjugants per donor.

3.2 Identification of ICE*Ml*Sym^{R7A} origin-of-transfer region

The relaxase RlxS is essential for transfer of ICE*Ml*Sym^{R7A} and extrachromosomal maintenance of ICE*Ml*Sym^{R7A} when excised (20). A hmmscan search (48) of relaxase protein family hmm profiles revealed RlxS was related to members of the MOB$_{P1}$ family (37, 38). *oriT* sites of MOB$_P$ relaxases generally contain an inverted-repeat sequence upstream of a conserved *nic* core region. *oriT* sites are often located upstream of their cognate relaxase gene (49, 50). To identify potential conserved sequence motifs upstream of the *rlxS* gene, the RlxS protein was used as a query in PSI-BLASTP searches (44) of non-mesorhizobial genomes. The NCBI-BLAST taxonomy viewer guided selection of a diverse collection of representatives from the PSI-BLASTP matches. Approximately 500-bp of DNA that preceded each relaxase was collected and analysed using MEME (43). MEME was set to search for 10-60-bp motifs present once on each sequence. Two large motifs were identified, which flanked an inverted-repeat which consisted of a variably-sized central region flanked by short regions of stronger conservation (**Fig. 2A**). One of the regions adjacent to the inverted-repeat bore resemblance to the consensus core region for MOB$_P$ relaxases and contained a conserved 'GC' *nic* sequence (**Fig. 2B**). Interestingly, an insertion sequence related to the IS*1111* family is present within this site in the *M. japonicum* MAFF303099 symbiosis-ICE sequence (**Fig. 2A**) (also noted in (28)), suggesting the MAFF303099 ICE may be non-mobile. It has been noted that members of the IS*1111* family preferentially target regions adjacent to DNA stem-loop structures for their insertion (35, 51-53).

3.3 *rlxS* and *rdfS* are essential for mobilisation of a plasmid carrying the ICE*Ml*Sym^{R7A} *oriT*

A 95-bp region encompassing the predicted *oriT* region was cloned into the broad host-range plasmid pFAJ1700, producing pFAJ2013. R7A(pFAJ2013) was used as a donor to mobilise pFAJ2013 by conjugation to *Escherichia coli* DC10B. pFAJ2013, but not the vector-only control pFAJ1700, was mobilised to DC10B at an average rate of 1.2×10^{-4} exconjugants per donor (**Table 2**). Next, pFAJ2013 was introduced into non-symbiotic derivative of R7A, R7ANS, and the *rlxS*-mutant R7A*rlxS*$^-$ (20) and the resulting strains were used as donors in conjugation experiments. No transfer was observed from either of these strains. To genetically complement the *rlxS* mutation, a region carrying both the *oriT* and the *rlxS* gene was cloned into pFAJ1700, producing plasmid pFAJCMV. In contrast to pFAJ2013, this plasmid was mobilised to *E. coli* from the R7A*rlxS*$^-$ background at an average frequency of 2.1×10^{-4} exconjugants per donor (**Table 2**). These data confirmed that mobilisation was dependent on the ICE*Ml*Sym^{R7A} conjugation machinery and *rlxS*.

rdfS is located directly upstream of the *oriT* and *rlxS*, suggesting it has evolved closely with the DNA transfer region of ICE*Ml*Sym^{R7A}. Therefore, we tested if a previously characterised strain carrying an in-frame deletion in *rdfS* (20) was able to mobilise pFAJ2013. Surprisingly, pFAJ2013 mobilisation was completely abolished in this background (**Table 2**). The lack of mobilisation was not related to a deficit in ICE*Ml*Sym^{R7A} excision per se, as pFAJ2013 transfer was observed from the *intS* mutant strain R7AΔ*intS* (in which ICE*Ml*Sym^{R7A} does not excise (20)), albeit at a reduced frequency. In order to complement the *rdfS* deletion, a vector compatible with pFAJ2013 was constructed, using pSRKKm (54). The *rdfS* coding sequence was placed downstream of the *lac* promoter in pSRKKm and the resulting plasmid pSRKrdfS was introduced into R7AΔ*rdfS*(pFAJ2013). To confirm pSRKrdfS was able to complement the ICE*Ml*Sym^{R7A} excision defect in R7AΔ*rdfS*, QPCR was carried out to measure the abundance of the excision products *attP* and *attB*. As expected, the R7AΔ*rdfS*(pFAJ2013)(pSRKKm) strain exhibited around 100-fold reduced abundance of *attP* and *attB* excision products compared to R7A carrying the same plasmids (**Supplemental Fig. 1**). Strain R7AΔ*rdfS*(pFAJ2013)(pSRKrdfS) however, exhibited close to wild-type levels of excision. Attempts to complement the deficit in pFAJ2013 transfer using the same strains were unsuccessful.

Table 2. Conjugation assay data and colony counts for pFAJ1700 vectors.

Strain	Vector	Region cloned	Transfer frequency[a]	Standard deviation
R7A	pFAJ1700		ND*	
	pFAJ2013	*oriT*	1.24×10^{-4}	2.62×10^{-5}
R7ANS	pFAJ1700		ND*	
	pFAJ2013	*oriT*	ND*	
R7A*rlxS*$^{-}$	pFAJ1700		ND*	
	pFAJ2013	*oriT*	ND*	
	pFAJCMV	*oriT-rlxS*	2.07×10^{-4}	6.29×10^{-5}
R7AΔ*intS*	pFAJ1700		ND*	
	pFAJ2013	*oriT*	7.12×10^{-6}	3.88×10^{-6}
	pFAJCMV	*oriT-rlxS*	6.64×10^{-6}	2.97×10^{-6}
R7AΔ*rdfS*	pFAJ1700		ND*	
	pFAJ2013	*oriT*	ND*	
	pFAJCMV	*oriT-rlxS*	ND*	

[a]Per-donor transfer frequencies are the average of three independent experiments.

*Not detected. Detection limit approximately 3.4×10^{-9}

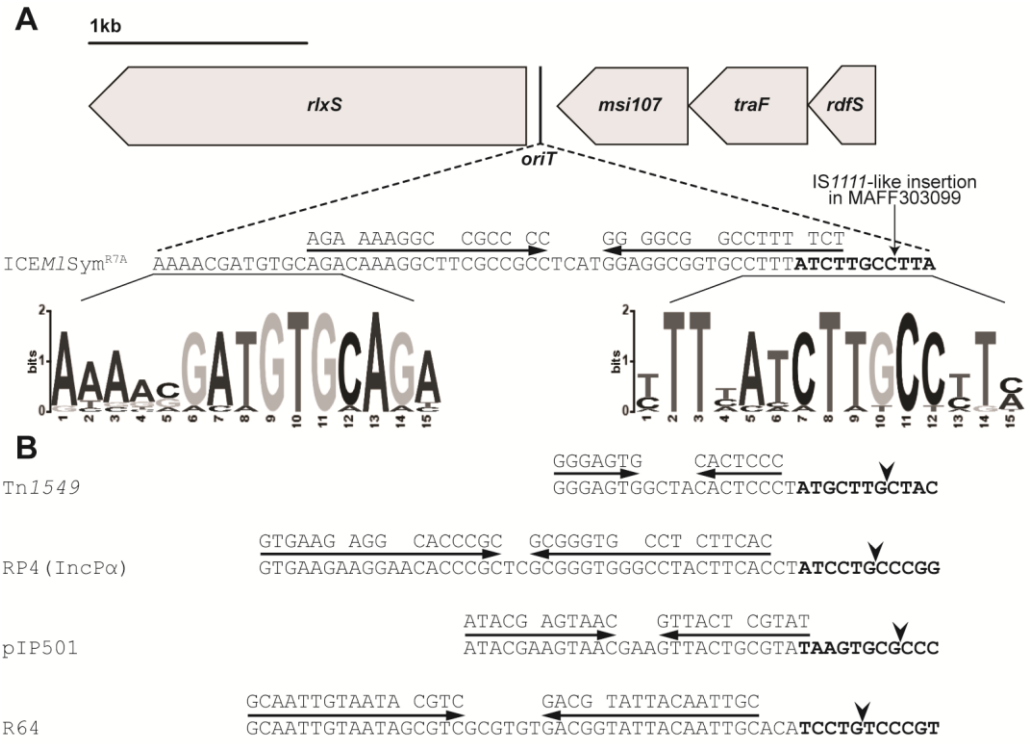

Fig. 2. The ICE*Ml*Sym^{R7A} origin-of-transfer (*oriT*).

(A) Organisation of *rdfS-rlxS* gene cluster, with relative location of *oriT* indicated (20, 28). Conserved sequences based on non-*Mesorhizobium* sp. relaxase-upstream regions (underlined) and inverted repeat location (arrows). Suspected *nic* core site bolded for ICE*Ml*Sym^{R7A} based on similarity to core sites shown in B. MEME-generated (43) 15-bp conserved motifs shown under respective underlined location. Location of IS*1111*-family transposon insertion within the related MAFF303099 ICE is indicated. (B) Inverted-repeat regions (arrows), partial *nic* core sites (bold) and *nic* sites (arrowhead) of *oriT* within MOB$_P$-carrying elements; conjugative transposon Tn*1549* (49), plasmid RP4 (IncP*α*) (55), pIP501 (56) and plasmid R64 (57).

4. DISCUSSION

Regulation of ICE*Ml*Sym^{R7A} excision and transfer has been extensively studied (9, 20, 58-60), however, the *cis*-acting sites integral to these processes, *attP* and the *oriT*, have remained relatively uncharacterised. In this work, we defined the minimal ICE*Ml*Sym^{R7A} *attP* region and showed that a 283-bp region containing five putative arm, or "P" sites, P1-P5, were sufficient for efficient integration by IntS. We also confirmed the location of the ICE*Ml*Sym^{R7A} *oriT* and demonstrated that a plasmid carrying the *oriT* region was mobilised from R7A to *E. coli* and this was dependent on the presence of ICE*Ml*Sym^{R7A} and *rlxS*.

Integrase P-site sequences and their positions relative to the core region vary but they are typically short, loosely conserved repeats positioned 50-140-bp from the *attP* core (11, 61) (**Fig. 3**). We identified a conserved 10-bp motif sequence following bioinformatic comparisons of putative *attL* sites from distantly related IntS-gene homologues. The consensus motif sequence “TGKTGGTATC” was present five times in each of the *attP* regions of ICE*Ml*Sym^{R7A}, ICE*Mc*Sym^{1271}, ICE*Ml*Sym^{2037} (32) and on putative ICEs in *Mesorhizobium* spp. strains WSM1284 and WSM1497. The arrangement of the likely P sites relative to the core site was similar to that observed for other well-characterised *attP* sites including Tn*916* and λ bacteriophage, despite the fact that these elements encode distantly related integrases (**Fig. 3**) (20, 62, 63). Removal of either of the outermost putative P sites significantly reduced the efficiency of integration, presumably due to reduced binding, or incorrect positioning of IntS molecules within the nucleoprotein complex during recombination (13, 14, 63). Integration was abolished when both outermost putative P sites were removed.

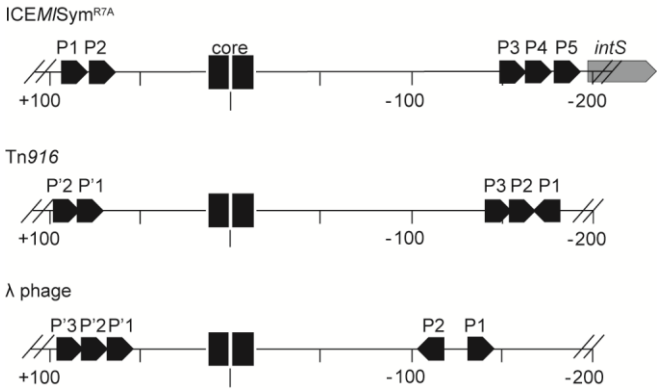

Fig. 3: **Comparison of the ICE*Ml*Sym^{R7A} *att* sites with those of Tn*916* and bacteriophage λ.**

Schematic of ICE*Ml*Sym^{R7A}, Tn*916* (34) and bacteriophage λ *attP* sites (63). Black lines representing each element are to scale, indicated below the DNA (in base-pairs relative to the core). The black rectangles show the *attP* site core regions (not to scale). Relative orientation of ICE*Ml*Sym^{R7A} putative P sites, and Tn*916* and bacteriophage λ P sites shown as the black arrows (not to scale). Start location of ICE*Ml*Sym^{R7A} IntS CDS shown with grey arrow.

RlxS is a member of the MOB_P family, a large and diverse family of relaxases found in a diverse collection of plasmids and ICEs. *oriT* sites of MOB_P relaxases typically display considerable sequence diversity, however they often contain a moderately conserved *nic* core sequence adjacent to a less conserved inverted-repeat region (49, 64). The ICE*Ml*Sym^{R7A} *oriT* region contained an inverted-repeat region and interestingly, strongly conserved motifs that flanked it were identified. One of these motifs resembled a MOB_P *nic* core site (**Fig. 2B**), however, it is possible that the core region could be positioned on the other side of the inverted repeat. Further work is required to fully dissect the functional components of the ICE*Ml*Sym^{R7A} *oriT*.

rdfS is peculiar for an RDF gene in that it is present upstream of genes involved in conjugation; *traF*, *msi107* (a lytic transglycosylase) and *rlxS*, rather than adjacent to its cognate integrase *intS* (28). Here we demonstrated that deletion of *rdfS* abolished the ability of the ICE*Ml*Sym^{R7A} conjugation system to mobilise a plasmid carrying the *oriT*. Strangely, ectopic expression of *rdfS* restored the excision defect observed in the *rdfS* mutant, as previously demonstrated (20), but did not restore the mobilisation defect (**Supplemental Fig. 1**). *rdfS* is the first gene in a polycistronic operon encoding *traF*, *msi107* and probably *rlxS* (33, 58). The *traF* start site also overlaps with the *rdfS* stop codon suggesting they may be translationally coupled. We cannot exclude the possibility that loss of mobilisation was due to disruption of downstream expression or translation of *traF* and/or *msi107*. However, the R7AΔ*rdfS* deletion is markerless, in-frame and the deletion terminates 59-bp upstream of the *traF* open-reading frame (20).

It is possible that RdfS is required for transcriptional activation of other conjugation genes on ICE*Ml*Sym^{R7A} such as the type-IV secretion system (*trb*) gene cluster or *rlxS*. We have previously demonstrated that RdfS activates expression of both *rdfG* and *rdfM* on ICE*Mc*Sym^{1271} (33), so a role for RdfS as a transcriptional activator of conjugation genes is conceivable. The TraN protein of the *Enterococcus sp.* plasmid pIP501, like RdfS, is a wHTH protein and it binds upstream of the pIP501 *oriT* and represses transcription of the *tra*-operon, repressing transfer (65, 66). Alternatively, RdfS could have a more direct role in *oriT* processing or relaxosome assembly. The *Clostridium perfringens* plasmid pCW3 encodes a wHTH transcription factor necessary for conjugation, TcpK, which binds the *oriT* utilising a novel binding mechanism for wHTH proteins (67). However, these possibilities aside, it remains unclear why mobilisation of pFAJ2013 was not restored by pSRKrdfS, unless the appropriate physiological levels of RdfS protein were not achieved using this vector. In future experiments investigating the downstream effects of the *rdfS* deletion, including possible polarity of the mutation on expression and translation of *traF* and *msi107*, will be required to resolve this.

ICE*Ml*Sym^{R7A} transfer requires coordination of IntS-mediated excision with expression of the type-IV secretion system and processing of the relaxosome. It is clear from the positioning of *rdfS* as the first gene in a cluster containing essential transfer genes *traF* and *rlxS* that coregulation of these processes has become linked over the course of evolution and our results suggest that they may be mechanistically intertwined. The work described herein defines the *attP* and *oriT* sites ICE*Ml*Sym^{R7A} and demonstrates a potentially complex link between the regulation of excision and transfer through expression of the *rdfS-traF-msi107* region.

DATA AVAILABILITY

All data have been provided in-text and accession numbers listed where appropriate.

SUPPLEMENTARY DATA

Supplemental Table 1: Bacterial strains and plasmids utilised in this study.

Supplemental Table 2: Oligonucleotides used in this study.

Supplemental Fig. 1: Excision percentages of R7A and *rdfS* mutant strains containing pFAJ2013 and pSRK or pSRKrdfS vectors.

ACKNOWLEDGEMENTS

CJV and JPR acknowledge technical support from the Curtin Health Innovation Research Institute.

FUNDING

JPR is the recipient of an Australian Research Council Future Fellowship [Project ID FT170100235] funded by the Australian Government (http://www.arc.gov.au/grants). CJV is the recipient of an Australian Government Research Training Program (RTP) Scholarship administered by the University of Western Australia. CJV and JPR received funding from the School of Pharmacy and Biomedical Sciences, Curtin University. Part of this work was supported by a grant from the Marsden Fund administered by the Royal Society of New Zealand.

CONFLICT OF INTEREST

The authors have declared that no competing interests exist.

REFERENCES

1. Burrus V, Pavlovic G, Decaris B, Guedon G. Conjugative transposons: the tip of the iceberg. Mol Microbiol. 2002;46:601-10. doi: 10.1046/j.1365-2958.2002.03191.x
2. Finan TM. Evolving Insights: Symbiosis Islands and Horizontal Gene Transfer. J Bacteriol. 2002;184:2855. doi: 10.1128/JB.184.11.2855-2856.2002
3. Johnson C, Grossman A. Integrative and Conjugative Elements (ICEs): What They Do and How They Work. Annual Rev Genet. 2015;49:577. doi: 10.1146/annurev-genet-112414-055018
4. Guglielmini J, Quintais L, Garcillán-Barcia MP, De La Cruz F, Rocha EPC. The repertoire of ICE in prokaryotes underscores the unity, diversity, and ubiquity of conjugation. PLoS Genet. 2011. doi: 10.1371/journal.pgen.1002222
5. Hochhut B, Waldor MK. Site‐specific integration of the conjugal *Vibrio cholerae* SXT element into *prfC*. Mol Microbiol. 1999;32:99-110. doi: 10.1046/j.1365-2958.1999.01330.x
6. Juhas M, van der Meer JR, Gaillard M, Harding RM, Hood DW, Crook DW. Genomic islands: tools of bacterial horizontal gene transfer and evolution. FEMS Microbiol Rev. 2009;33:376-93. doi:10.1111/j.1574-6976.2008.00136.x
7. Rice LB. Tn916 Family Conjugative Transposons and Dissemination of Antimicrobial Resistance Determinants. Antimicrob Agents Chemother. 1998;42:1871-7. doi: 10.1128/AAC.42.8.1871
8. Schmidt H, Hensel M. Pathogenicity islands in bacterial pathogenesis. Clin Microbiol Rev. 2004;17:14-56. doi: 10.1128/CMR.17.1.14-56.2004
9. Sullivan J, Ronson C. Evolution of rhizobia by acquisition of a 500-kb symbiosis island that integrates into a *phe*-tRNA gene. Proc Natl Acad Sci USA. 1998;95:5145-9.
10. Bi D, Xu Z, Harrison EM, Tai C, Wei Y, He X, Jia S, Deng Z, Rajakumar K, Ou H-Y. ICEberg: a web-based resource for integrative and conjugative elements found in Bacteria. Nucleic Acids Res. 2012;40:D621-D6. doi: 10.1093/nar/gkr846
11. Groth AC, Calos MP. Phage Integrases: Biology and Applications. J Mol Biol. 2004;335:667-78. doi: 10.1016/j.jmb.2003.09.082
12. Lewis JA, Hatfull GF. Control of directionality in integrase-mediated recombination: examination of recombination directionality factors (RDFs) including Xis and Cox proteins. Nucleic Acids Res. 2001;29:2205. doi: 10.1093/nar/29.11.2205
13. Ravatn R, Studer S, Zehnder AJB, Roelof van der Meer J. Int- B13, an Unusual Site- Specific Recombinase of the Bacteriophage P4 Integrase Family, Is Responsible for Chromosomal Insertion of the 105- Kilobase *clc* Element of *Pseudomonas* sp. Strain B13. J Bacteriol. 1998;180:5505.
14. Campbell AM. Chromosomal insertion sites for phages and plasmids. J Bacteriol. 1992;174:7495. doi: 10.1128/jb.174.23.7495-7499.1992
15. Hirano N, Muroi T, Takahashi H, Haruki M. Site-specific recombinases as tools for heterologous gene integration. Appl Microbiol Biotechnol. 2011;92:227-39. doi: 10.1007/s00253-011-3519-5
16. Esposito D, Scocca JJ. The integrase family of tyrosine recombinases: evolution of a conserved active site domain. Nucleic Acids Res. 1997;25:3605.
17. Hazelbaker D, Azaro MA, Landy A. A biotin interference assay highlights two different asymmetric interaction profiles for lambda integrase arm-type binding sites in integrative versus excisive recombination. J Biol Chem. 2008;283:12402-14. doi: 10.1074/jbc.M800544200
18. Radman-Livaja M, Biswas T, Mierke D, Landy A. Architecture of recombination intermediates visualized by in-gel FRET of λ integrase-Holliday junction-arm DNA complexes. Proc Natl Acad Sci USA. 2005;102:3913-20. doi: 10.1073/pnas.0500844102
19. Rachel AFW, Matthew KW. Integrative and conjugative elements: mosaic mobile genetic elements enabling dynamic lateral gene flow. Nat Rev Microbiol. 2010;8:552. doi: 10.1038/nrmicro2382

20. Ramsay JP, Sullivan JT, Stuart GS, Lamont IL, Ronson CW. Excision and transfer of the *Mesorhizobium loti* R7A symbiosis island requires an integrase IntS, a novel recombination directionality factor RdfS, and a putative relaxase RlxS. Mol Microbiol. 2006;62:723-34. doi: 10.1111/j.1365-2958.2006.05396.x
21. Lundqvist B, Bertani G. Immunity repressor of bacteriophage P2. Identification and DNA-binding activity. J Mol Biol. 1984;178:629-51. doi: 10.1016/0022-2836(84)90242-0
22. Dodd IB, Kalionis B, Egan JB. Control of gene expression in the temperate coliphage 186. VIII. Control of lysis and lysogeny by a transcriptional switch involving face-to-face promoters. J Mol Biol. 1990;214:27-37. doi: 10.1016/0022-2836(90)90144-b
23. Reed MR, Shearwin KE, Pell LM, Egan JB. The dual role of Apl in prophage induction of coliphage 186. Mol Microbiol. 1997;23:669-81. doi: 10.1002/j.1460-2075.1987.tb02631.x
24. Esposito D, Wilson JC, Scocca JJ. Reciprocal regulation of the early promoter region of bacteriophage HP1 by the Cox and Cl proteins. Virology. 1997;234:267-76. doi: 10.1006/viro.1997.8646
25. Saha S, Haggård-Ljungquist E, Nordström K. Activation of prophage P4 by the P2 Cox protein and the sites of action of the Cox protein on the two phage genomes. Proc Natl Acad Sci U S A. 1989;86:3973-7. doi: 10.1073/pnas.86.11.3973
26. Saha S, Haggard-Ljungquist E, Nordstrom K. The cox protein of bacteriophage P2 inhibits the formation of the repressor protein and autoregulates the early operon. Embo j. 1987;6:3191-9.
27. Ahlgren-Berg A, Cardoso-Palacios C, Eriksson JM, Mandali S, Sehlen W, Sylwan L, Haggard-Ljungquist E. A comparative analysis of the bifunctional Cox proteins of two heteroimmune P2-like phages with different host integration sites. Virology. 2009;385:303-12. doi: 10.1016/j.virol.2008.12.002
28. Sullivan JT, Trzebiatowski JR, Cruickshank RW, Gouzy J, Brown SD, Elliot RM, Fleetwood DJ, McCallum NG, Rossbach U, Stuart GS, Weaver JE, Webby RJ, de Bruijn FJ, Ronson CW. Comparative Sequence Analysis of the Symbiosis Island of *Mesorhizobium loti* Strain R7A. J Bacteriol. 2002;184:3086. doi: 10.1128/JB.184.11.3086-3095.2002
29. Haskett T, Wang P, Ramsay J, O'Hara G, Reeve W, Howieson J, Terpolilli J. Complete Genome Sequence of *Mesorhizobium ciceri* bv. biserrulae Strain WSM1284, an Efficient Nitrogen-Fixing Microsymbiont of the Pasture Legume *Biserrula pelecinus*. Genome Announc. 2016;4. doi: 10.1128/genomeA.00514-16
30. Ling J, Wang H, Wu P, Li T, Tang Y, Naseer N, Zheng H, Masson-Boivin C, Zhong Z, Zhu J. Plant nodulation inducers enhance horizontal gene transfer of *Azorhizobium caulinodans* symbiosis island. Proc Natl Acad Sci USA. 2016;113:13875-80. doi: 10.1073/pnas.1615121113
31. Haskett TL, Ramsay JP, Bekuma AA, Sullivan JT, O'Hara GW, Terpolilli JJ. Evolutionary persistence of tripartite integrative and conjugative elements. Plasmid. 2017;92:30-6. doi: 10.1016/j.plasmid.2017.06.001
32. Haskett TL, Terpolilli JJ, Bekuma A, O'Hara GW, Sullivan JT, Wang P, Ronson CW, Ramsay JP. Assembly and transfer of tripartite integrative and conjugative genetic elements. Proc Natl Acad Sci USA. 2016;113:12268. doi: 10.1073/pnas.1613358113
33. Haskett TL, Terpolilli JJ, Ramachandran VK, Verdonk CJ, Poole PS, O'Hara GW, Ramsay JP. Sequential induction of three recombination directionality factors directs assembly of tripartite integrative and conjugative elements. PLoS Genet. 2018;14:e1007292. doi: 10.1371/journal.pgen.1007292
34. Abbani M, Iwahara M, Clubb RT. The Structure of the Excisionase (Xis) Protein from Conjugative Transposon Tn*916* Provides Insights into the Regulation of Heterobivalent Tyrosine Recombinases. J Mol Biol. 2005;347:11-25. doi: 10.1016/j.jmb.2005.01.019
35. Lanka E, Wilkins BM. DNA processing reactions in bacterial conjugation. Annu Rev Biochem. 1995;64:141-69. doi: 10.1146/annurev.bi.64.070195.001041
36. Llosa M, Gomis-Ruth FX, Coll M, de la Cruz Fd F. Bacterial conjugation: a two-step mechanism for DNA transport. Mol Microbiol. 2002;45:1-8. doi: 10.1046/j.1365-2958.2002.03014.x

37. Cabezon E, Ripoll-Rozada J, Pena A, de la Cruz F, Arechaga I. Towards an integrated model of bacterial conjugation. FEMS Microbiol Rev. 2015;39:81-95. doi: 10.1111/1574-6976.12085
38. Green ER, Mecsas J. Bacterial Secretion Systems: An Overview. Microbiol Spectr. 2016;4:10.1128/microbiolspec.VMBF-0012-2015. doi: 10.1128/microbiolspec.VMBF-0012-2015
39. Chandran Darbari V, Waksman G. Structural Biology of Bacterial Type IV Secretion Systems. Annu Rev Biochem. 2015;84:603-29. doi: 10.1146/annurev-biochem-062911-102821
40. Ronson CW, Nixon BT, Albright LM, Ausubel FM. *Rhizobium meliloti ntrA* (*rpoN*) gene is required for diverse metabolic functions. J Bacteriol. 1987;169:2424-31. doi: 10.1128/jb.169.6.2424-2431.1987
41. Monk IR, Shah IM, Xu M, Tan M-W, Foster TJ. Transforming the Untransformable: Application of Direct Transformation To Manipulate Genetically *Staphylococcus aureus* and *Staphylococcus epidermidis*. mBio. 2012;3:3824. doi: 10.1128/mBio.00277-11
42. Hubber A, Vergunst AC, Sullivan JT, Hooykaas PJ, Ronson CW. Symbiotic phenotypes and translocated effector proteins of the *Mesorhizobium loti* strain R7A VirB/D4 type IV secretion system. Mol Microbiol. 2004;54:561-74. doi: 10.1111/j.1365-2958.2004.04292.x
43. Bailey TL, Boden M, Buske FA, Frith M, Grant CE, Clementi L, Ren J, Li WW, Noble WS. MEME Suite: tools for motif discovery and searching. Nucleic Acids Res. 2009;37:W202-W8. doi: 10.1093/nar/gkp335
44. Altschul SF, Madden TL, Schaffer AA, Zhang J, Zhang Z, Miller W, Lipman DJ. Gapped BLAST and PSI-BLAST: a new generation of protein database search programs. Nucleic Acids Res. 1997;25:3389-402. doi: 10.1093/nar/25.17.3389
45. Bailey TL, Elkan C. Fitting a mixture model by expectation maximization to discover motifs in biopolymers. Proc Int Conf Intell Syst Mol Biol. 1994;2:28-36.
46. Zimmermann L, Stephens A, Nam SZ, Rau D, Kubler J, Lozajic M, Gabler F, Soding J, Lupas AN, Alva V. A Completely Reimplemented MPI Bioinformatics Toolkit with a New HHpred Server at its Core. J Mol Biol. 2018;430:2237-43. doi: 10.1016/j.jmb.2017.12.007
47. Thoma S, Schobert M. An improved *Escherichia coli* donor strain for diparental mating. FEMS Microbiol Lett. 2009;294:127-32. doi: 10.1111/j.1574-6968.2009.01556.x
48. Eddy SR. A Probabilistic Model of Local Sequence Alignment That Simplifies Statistical Significance Estimation. PLOS Comput Biol. 2008;4:e1000069. doi: 10.1371/journal.pcbi.1000069
49. Tsvetkova K, Marvaud JC, Lambert T. Analysis of the mobilization functions of the vancomycin resistance transposon Tn*1549*, a member of a new family of conjugative elements. J Bacteriol. 2010;192:702-13. doi: 10.1128/jb.00680-09
50. Francia MV, Varsaki A, Garcillan-Barcia MP, Latorre A, Drainas C, de la Cruz F. A classification scheme for mobilization regions of bacterial plasmids. FEMS Microbiol Rev. 2004;28:79-100. doi: 10.1016/j.femsre.2003.09.001
51. Parker C, Becker E, Zhang X, Jandle S, Meyer R. Elements in the co-evolution of relaxases and their origins of transfer. Plasmid. 2005;53:113-8. doi: 10.1016/j.plasmid.2004.12.007
52. de la Cruz F, Frost LS, Meyer RJ, Zechner EL. Conjugative DNA metabolism in Gram-negative bacteria. FEMS Microbiol Rev. 2010;34:18-40. doi: 10.1111/j.1574-6976.2009.00195.x
53. Partridge SR, Hall RM. The IS*1111* Family Members IS*4321* and IS*5075* Have Subterminal Inverted Repeats and Target the Terminal Inverted Repeats of Tn*21* Family Transposons. J Bacteriol. 2003;185:6371. doi: 10.1128/JB.185.21.6371-6384.2003
54. Khan SR, Gaines J, Roop RM, 2nd, Farrand SK. Broad-host-range expression vectors with tightly regulated promoters and their use to examine the influence of TraR and TraM expression on Ti plasmid quorum sensing. Applied and environmental microbiology. 2008;74:5053-62. doi: 10.1128/AEM.01098-08
55. Pansegrau W, Lanka E. Mechanisms of initiation and termination reactions in conjugative DNA processing. Independence of tight substrate binding and catalytic activity of relaxase (TraI) of IncPalpha plasmid RP4. J Biol Chem. 1996;271:13068-76. doi: 10.1074/jbc.271.22.13068

56. Wang A, Macrina FL. Streptococcal plasmid pIP501 has a functional *oriT* site. J Bacteriol. 1995;177:4199-206. doi: 10.1128/jb.177.15.4199-4206.1995
57. Furuya N, Komano T. Mutational analysis of the R64 *oriT* region: requirement for precise location of the NikA-binding sequence. J Bacteriol. 1997;179:7291-7. doi: 10.1128/jb.179.23.7291-7297.1997
58. Ramsay JP, Major AS, Komarovsky VM, Sullivan JT, Dy RL, Hynes MF, Salmond GPC, Ronson CW. A widely conserved molecular switch controls quorum sensing and symbiosis island transfer in *Mesorhizobium loti* through expression of a novel antiactivator. Mol Microbiol. 2013;87:1-13. doi: 10.1111/mmi.12079
59. Ramsay JP, Sullivan JT, Jambari N, Ortori CA, Heeb S, Williams P, Barrett DA, Lamont IL, Ronson CW. A LuxRI‐family regulatory system controls excision and transfer of the *Mesorhizobium loti* strain R7A symbiosis island by activating expression of two conserved hypothetical genes. Mol Microbiol. 2009;73:1141-55. doi: 10.1111/j.1365-2958.2009.06843.x
60. Ramsay JP, Tester LGL, Major AS, Sullivan JT, Edgar CD, Kleffmann T, Patterson-House JR, Hall DA, Tate WP, Hynes MF, Ronson CW. Ribosomal frameshifting and dual-target antiactivation restrict quorum-sensing-activated transfer of a mobile genetic element. Proc Natl Acad Sci USA. 2015;112:4104. doi: 10.1073/pnas.1501574112
61. Raynal A, Friedmann A, Tuphile K, Guerineau M, Pernodet J. Characterization of the *attP* site of the integrative element pSAM2 from *Streptomyces ambofaciens*. Microbiology. 2002;148:61-7. doi: 10.1099/00221287-148-1-61
62. Poyart-Salmeron C, Trieu-Cuot P, Carlier C, Courvalin P. Molecular characterization of two proteins involved in the excision of the conjugative transposon Tn*1545*: homologies with other site-specific recombinases. Embo j. 1989;8:2425-33.
63. Bushman W, Thompson JF, Vargas L, Landy A. Control of directionality in lambda site specific recombination. Science. 1985;230:906-11.
64. Garcillan-Barcia MP, Francia MV, de la Cruz F. The diversity of conjugative relaxases and its application in plasmid classification. FEMS Microbiol Rev. 2009;33:657-87. doi: 10.1111/j.1574-6976.2009.00168.x
65. Goessweiner‐Mohr N, Eder M, Hofer G, Fercher C, Arends K, Birner‐Gruenberger R, Grohmann E, Keller W. Structure of the double‐stranded DNA‐binding type IV secretion protein TraN from *Enterococcus*. Acta Crystallogr Sect D. 2014;70:2376-89. doi: 10.1107/S1399004714014187
66. Kohler V, Goessweiner-Mohr N, Aufschnaiter A, Fercher C, Probst I, Pavkov-Keller T, Hunger K, Wolinski H, Buttner S, Grohmann E, Keller W. TraN: A novel repressor of an *Enterococcus* conjugative type IV secretion system. Nucleic Acids Res. 2018;46:9201-19. doi: 10.1093/nar/gky671
67. Traore DAK, Wisniewski JA, Flanigan SF, Conroy PJ, Panjikar S, Mok Y-F, Lao C, Griffin MDW, Adams V, Rood JI, Whisstock JC. Crystal structure of TcpK in complex with *oriT* DNA of the antibiotic resistance plasmid pCW3. Nat Commun. 2018;9:3732. doi: 10.1038/s41467-018-06096-2

HIGHLIGHTS

Verdonk, CJ, *et al.* **Delineation of the integrase-attachment and origin-of-transfer regions of the symbiosis island ICE*Ml*Sym^{R7A}**

- We define the minimal ICE*Ml*Sym^{R7A} integrase attachment site *attP* region sufficient for efficient IntS-mediated integration
- We define the origin-of-transfer (*oriT*) region for ICE*Ml*Sym^{R7A}
- The ICE*Ml*Sym^{R7A} conjugation system can mobilise an *oriT*-carrying plasmid to *Escherichia coli*